A Stochastic Approach to the Response of Torsionally Coupled Multistoried Buildings

Pavan Agarwal*, Vinay K. Gupta**

SUMMARY – A stochastic approach based on the response spectrum superposition technique has been formulated to determine the linear lateral-torsional response of torsionally coupled multistoried buildings subjected to the earthquake excitations. The eccentricity between the centres of mass and stiffness is assumed to cause the coupling between the lateral and torsional responses of the building. The key features of this approach are: 1) it can estimate the response peaks for all orders with the given level of confidence, 2) it accounts for the cross-correlation between various modes of vibration in a simple and convenient way, and 3) no assumption is made about the energy distribution in the incoming seismic waves. The proposed approach has been illustrated through two example buildings and two narrow and wide-band type earthquake excitations.

KEYWORDS:

1. Introduction

Buildings are seldom, if ever totally symmetric, due to the unsymmetrical distribution of mass and/or stiffness in the plan. Even in a structure whose geometry is symmetric, asymmetry is introduced by the variation in quality or method of construction, or by uncertainties in the live and dead load distribution. This asymmetry in the buildings causes the positions of centre of mass and centre of stiffness to be different, and thus results in significant coupling between the translational and the torsional vibrations of the structure even when the earthquake excitation is in the form of a uniform base translation. As a result of the coupled lateral-torsional response, the induced lateral and torsional forces acting on the asymmetric buildings can, in combination, exceed design values to an extent which would result in wide-spread damage or failure of buildings. Chandler (1986) found that during the Mexico Earthquake, 1985, 15 percent of the cases of severe damage or collapse of buildings in Mexico City were caused by the pronounced asymmetry in stiffness. Torsional response results also from the non-uniform ground motion at various points of the base of the building. However, as shown by Gupta and Trifunac (1990b) in case of the fixed-base, symmetric multistoried buildings, this may be considered insignificant.

Several studies have been directed towards the linear earthquake analysis of fixed-base, torsionally coupled buildings. Dempsey and Tso (1982), Chandler and Hutchinson (1986, 1987) have used the time-history approach for the study of seismic torsional effects in asymmetrical buildings. Tsicnias and Hutchinson (1981, 1982a), Kan and Chopra (1977a), Tso and Dempsey (1980), Dempsey and Irvine (1979) have idealized the spectral acceleration curves as flat, hyperbolic or flat-hyperbolic. These idealizations are however unsuitable for drawing general conclusions on coupling effects in the asymmetric buildings, and may sometimes lead to 'too approximate' results (Hejal and Chopra (1989a)). Kan and Chopra (1977b) and Tsicnias and Hutchinson (1982b) applied the perturbation analysis for the determination of approximate natural frequencies and mode shapes of the torsionally coupled buildings. Other investigators who also studied the torsional response of linear, asymmetric buildings, include Penzien (1969), Gibson et al. (1972), Douglas and Trabert (1973), Keintzel (1973), Rutenberg et al. (1978), Lam and Scavuzzo (1981), Hejal and Chopra (1989b), and Maheri et al. (1991).

In most of the studies, various simple response spectrum techniques have been used to obtain the deterministic estimates of the structural response. To account for the uncertainties involved in defining the earthquake motions, a few studies have also considered the stochastic models of ground motion. Kung and Pecknold

* Engineer, Engineers India Limited, New Delhi, India.
** Associate Professor, Dept. of Civil Engineering, Indian Institute of Technology, Kanpur – 208016, India.
Received november 1994. Revised april 1995.

(1984) assumed the ground motion to be a white noise input. Rady and Hutchinson (1988) used a more realistic ground acceleration power spectrum to study the response of torsionally coupled structures. However, due to the limitation of these studies to a single story model, their results cannot be generalized to the multistoried buildings. Hutchinson et al. (1991) have used the stochastic approach to study the effects of vertical mass and stiffness distribution only for a special class of multistoried buildings.

None of the above studies on the torsionally coupled buildings have provided the amplitudes of the higher order response peaks. This knowledge is useful for better understanding of the progressing damage, as the structure is subjected to the successive excursions beyond the design level during the excitation (Basu and Gupta (1994)). Many studies (Amini and Trifunac (1981, 1985), Gupta and Trifunac (1987b, 1988), Gupta and Trifunac (1990a, c, 1991)) based on a torsionally uncoupled model of the building have used the ideas of order statistics to provide amplitudes of all the significant peaks of the response with the desired level of confidence. This paper proposes to extend their approach for estimating the response peaks of linear, fixed-base, torsionally coupled multistoried buildings subjected to the single component of the ground excitation. A lumped mass model of the building, having three degrees of freedom at each floor, has been considered for this purpose. This approach is quite general as it is suitable for the earthquake excitations with varying characteristics, including the narrow band excitations, and for the structures with closely spaced modes of vibration. By taking the examples of two buildings and two different seismic excitations, the proposed approach has been illustrated.

2. Brief Review

The statistical distribution of peak amplitudes in a stationary random process has been studied initially by Rice (1944, 1945), and Cartwright and Longuet-Higgins (1956). Gupta and Trifunac (1988) used their results to derive the general distribution functions for the various orders of peaks by assuming that the unordered peaks are statistically independent. It has been shown recently by Basu et al. (1994) through modeling of the joint density between the unordered peaks by numerical simulation that this assumption of statistical independence gives quite reasonable estimates for the first few orders of peaks. Using the formulation of Gupta and Trifunac (1988), a response spectrum superposition technique has been formulated for the stochastic response of symmetric multistoried buildings subjected to the earthquake excitations (Gupta and Trifunac (1987a, b, 1988), Gupta and Trifunac (1990a, c, 1991)). For these applications, a torsionally uncoupled, simple lumped mass model has been considered. Some of the key features of these are as follows.

Let the random function, $f(t)$, e.g., the response of a structure to an earthquake excitation be represented by the sum of an infinite number of sine waves as

$$f(t)=\sum_n cn\cos(\omega_n t+\phi_n), \tag{2.1}$$

where ω_n are the circular frequencies, ϕ_n are the random, uniformly distributed phases, and c_n are the amplitudes such that

$$\sum_{\omega_n=\omega}^{\omega+d\omega}\frac{1}{2}c_n^2=E(\omega)d\omega. \tag{2.2}$$

Here, $E(\omega)$ is the energy spectrum of $f(t)$. This may be related to the Fourier spectrum, $F(\omega)$ of the function $f(t)$ as (Udwadia and Trifunac (1974), Mohraz and Elghadamsi (1989))

$$E(\omega)=\frac{1}{\pi T}|F(\omega)|^2, \tag{2.3}$$

where, T is the total duration of the response.

Let all the N peaks of $f(t)$ be normalized with respect to a_{rms}, the root-mean-square (r.m.s.) amplitude of $f(t)$. Then, the n^{th} order peak (in decreasing order of magnitude) in these normalized peaks with $n \le N$ is distributed as (Gupta and Trifunac (1988)),

$$p_{(n)}(\eta)=\frac{N!}{(N-n)!(n-1)!}[P(\eta)]^{n-1}[1-P(\eta)]^{N-n}p(\eta). \tag{2.4}$$

$P(\eta)$ is the probability distribution function of the (normalized) maxima of $f(t)$, expressed as (Cartwright and Longuet-Higgins (1956))

$$P(\eta)=\frac{1}{\sqrt{2\pi}}\left[\int_{\eta/\epsilon}^{\infty}e^{-x^2/2}\mathrm{d}x+ +(1-\epsilon^2)^{1/2}e^{-\eta^2/2}\int_{-\infty}^{\eta(1-\epsilon^2)^{1/2}/\epsilon}e^{-x^2/2}\mathrm{d}x\right], \tag{2.5}$$

and

$$p(\eta)=-\frac{\mathrm{d}P(\eta)}{\mathrm{d}\eta}. \tag{2.6}$$

Here, ϵ is a measure of the r.m.s. width of the energy spectrum, $E(\omega)$. The parameters, a_{rms} and ϵ are defined in terms of the moments, m_n, n = 0, 2, 4 of $E(\omega)$ as

$$a_{rms}=\sqrt{m_0} \tag{2.7}$$

and

$$\epsilon=\left[1-\frac{m_2^2}{m_0 m_4}\right]^{1/2}, \tag{2.8}$$

with

$$m_n=\int_0^{\infty}\omega^n E(\omega)d\omega. \tag{2.9}$$

The total number of peaks in $f(t)$ is

$$N = \frac{T}{2\pi}\left(\frac{m_4}{m_2}\right)^{1/2}. \quad (2.10)$$

For a given confidence level, Eq. (2.4) may be iteratively used to find the peak factor, η which on being multiplied with a_{rms} gives the n^{th} order peak amplitude. For the «expected» peak amplitude, the peak factor, $\eta = \overline{\eta}$ may be computed as

$$\overline{\eta} = \int_{-\infty}^{\infty} \eta p_{(n)}(\eta) \mathrm{d}\eta. \quad (2.11)$$

The integral in this equation may be obtained by an approximate approach given by David and Johnson (1954), and also used later by Gupta and Trifunac (1988). If the peaks of $f(t)$ are normalized with respect to their r.m.s. value, $\overline{a}$ (in place of a_{rms}), $\eta/\sqrt{2}$ denotes (in place of η) the peak factor since $\overline{a}$ can be shown to be approximately equal to $\sqrt{2}a_{rms}$ for the narrow band processes (Udwadia and Trifunac (1973)). It is also possible to obtain more appropriate peak factors (as regards the applications in earthquake engineering) for the process, $|f(t)|$ by slightly modifying Eqs. (2.4), (2.5) and (2.10) as in Gupta (1994).

Since the r.m.s. value of response peaks is calculated above assuming the response to be a stationary process, Gupta and Trifunac (1987b) have suggested to modify this for the nonstationarity by using the response spectrum amplitudes. It has been proposed that the r.m.s. value of the peaks instead be taken as $\tilde{a}$ where

$$\tilde{a} = \left[\sum_{j=1}^{n} \tilde{a}_j^2\right]^{1/2}. \quad (2.12)$$

$\tilde{a}_j$ is the r.m.s. value such that on multiplication with the peak factor computed for the expected value of the first order peak, it gives the largest peak value in the j^{th} mode as obtained from the response spectrum.

The above procedure can be applied to estimate the stochastic response of any response function in a linear dynamic system from the knowledge of its energy spectrum in addition to the response spectrum. This however does not consider the effects of interaction between various modes of vibration on the value of $\tilde{a}$. Gupta and Trifunac (1990a, c) have shown that these effects can however be included in a simple and approximate manner by scaling $\tilde{a}$ in that ratio in which $\tilde{a}$ is modified on including the interaction terms in the energy spectrum.

3. Equations of Motion

Let us consider an idealized n-story unsymmetric building model as shown in Fig. 1. It consists of rigid floor decks which are supported on massless, axially inextensible columns and shear walls. Following assumptions are made for the present formulation:

i) The inertia of the i^{th} floor is lumped at that level by a mass, m_i and by a mass moment of inertia, I_i, about the centre of mass of the floor;

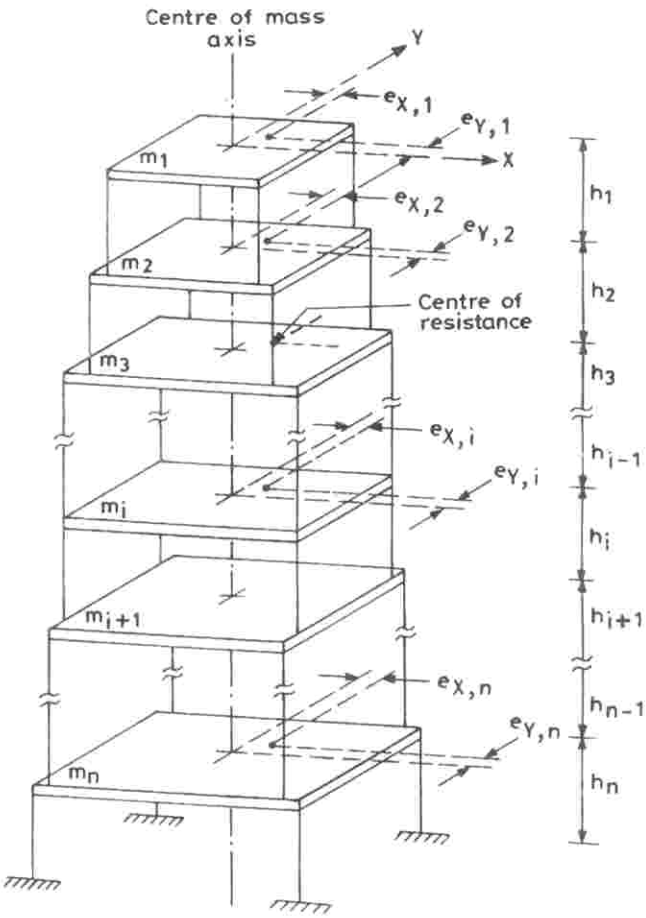

Fig. 1 – Multi-Degree-of-Freedom System for Torsionally Coupled Buildings.

ii) The linear rigidities of the i^{th} story are provided by the massless columns and shear walls, and these are characterized by the three constants, the lateral stiffnesses, $K_{X,i}$ and $K_{Y,i}$ along the X and Y-axes, and the torsional stiffness, $K_{\theta,i}$ about the vertical Z-axis, passing through the centre of mass. It is also assumed that the principal axes of resistance for all the story levels are parallel to the X and Y-axes.

iii) The centres of mass of the floors lie on one vertical axis, which coincides with the Z-axis, but the centres of stiffness of the stories lie on different vertical axes, with static eccentricities, $e_{X,i}$ and $e_{Y,i}$ respectively along the X and Y-axes for the i^{th} story as shown in Fig. 2.

The ground motion is assumed to be in X-direction only. This system has three degrees of freedom for each floor, e.g., X-direction translation, V_{Xi}, Y-direction translation, V_{Yi}, and rotation about the centre of mass, $V_{\theta i}$ at the i^{th} floor level (see Fig. 2). The equations of motion for the above building model can be expressed as

$$[M]\{\ddot{V}\}+[C]\{\dot{V}\}+[K]\{V\} = -[M]\{\gamma\}\ddot{Z}_X \quad (3.1)$$

in which, $[M]$, $[C]$ and $[K]$ are the inertia, damping and stiffness matrices respectively; $\{V\}$ is the $3n$-dimensional relative displacement vector; $\ddot{Z}_X$ is the ground acceleration in X-direction; and $\{\gamma\}$ is the influence

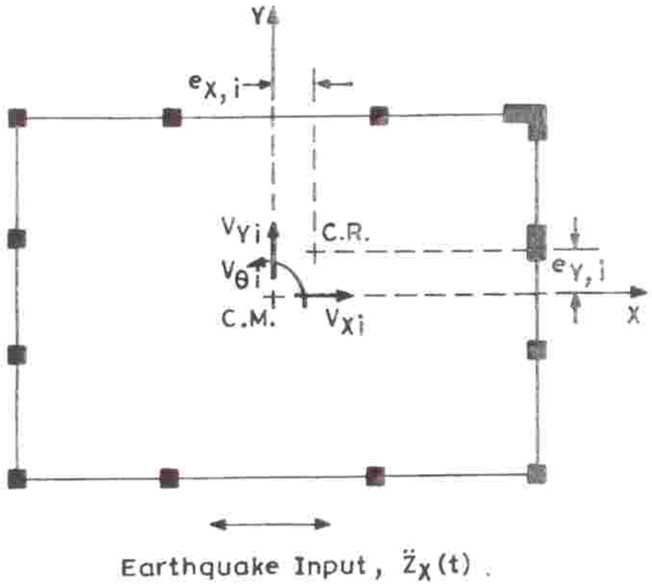

Fig. 2 - Plan of the i[th] Floor level of the Building.

vector for various degrees of freedom. Eq. (3.1) can be represented as (Kan and Chopra (1977b)):

$$\begin{bmatrix} [m] & & \\ & [m] & \\ & & [m] \end{bmatrix} \begin{Bmatrix} \{\ddot{V}_X\} \\ \{\ddot{V}_Y\} \\ \{\ddot{V}_\theta\} \end{Bmatrix} + [C] \begin{Bmatrix} \{\dot{V}_X\} \\ \{\dot{V}_Y\} \\ \{\dot{V}_\theta\} \end{Bmatrix} +$$

$$\begin{bmatrix} [\mathbf{K}_X] & [0] & [\mathbf{K}_{X\theta}] \\ [0] & [K_Y] & [\mathbf{K}_{Y\theta}] \\ [\mathbf{K}_{X\theta}]^T & [\mathbf{K}_{Y\theta}]^T & [\mathbf{K}_\theta] \end{bmatrix} \begin{Bmatrix} \{V_X\} \\ \{V_Y\} \\ \{V_\theta\} \end{Bmatrix} = \qquad (3.2)$$

$$-\begin{bmatrix} [m] & & \\ & [m] & \\ & & [m] \end{bmatrix} \begin{Bmatrix} \{1\} \\ \{0\} \\ \{0\} \end{Bmatrix} \ddot{Z}_X,$$

where,

$$[m] = \begin{bmatrix} m_1 & & & & & \\ & m_2 & & & & \\ & & \ddots & & & \\ & & & m_i & & \\ & & & & \ddots & \\ & & & & & m_n \end{bmatrix}$$

$$[\mathbf{K}_X] = \begin{bmatrix} K_{X,1} & -K_{X,1} & & & \\ -K_{X,1} & (K_{X,1}+K_{X,2}) & -K_{X,2} & & \\ & -K_{X,2} & (K_{X,2}+K_{X,3}) & \ddots & \\ & & \ddots & \ddots & -K_{X,n-1} \\ & & & -K_{X,n-1} & (K_{X,n-1}+K_{X,n}) \end{bmatrix}$$

$$[\mathbf{K}_Y] = \begin{bmatrix} K_{Y,1} & -K_{Y,1} & & & \\ -K_{Y,1} & (K_{Y,1}+K_{Y,2}) & -K_{Y,2} & & \\ & -K_{Y,2} & (K_{Y,2}+K_{Y,3}) & \ddots & \\ & & \ddots & \ddots & -K_{Y,n-1} \\ & & & -K_{Y,n-1} & (K_{Y,n-1}+K_{Y,n}) \end{bmatrix}$$

$$[\mathbf{K}_\theta] = \begin{bmatrix} \left(\frac{1}{r_1}\right)^2 K_{\theta,1} & -\frac{1}{r_1 r_2} K_{\theta,1} & & & \\ -\frac{1}{r_1 r_2} K_{\theta,1} & \left(\frac{1}{r_2}\right)^2 (K_{\theta,1}+K_{\theta,2}) & -\frac{1}{r_2 r_3} K_{\theta,2} & & \\ & -\frac{1}{r_2 r_3} K_{\theta,2} & \left(\frac{1}{r_3}\right)^2 (K_{\theta,2}+K_{\theta,3}) & \ddots & \\ & \ddots & \ddots & & -\frac{1}{r_{n-1} r_n} K_{\theta,n-1} \\ & & & -\frac{1}{r_{n-1} r_n} K_{\theta,n-1} & \left(\frac{1}{r_n}\right)^2 (K_{\theta,n-1}+K_{\theta,n}) \end{bmatrix}$$

$$[\mathbf{K}_{X\theta}] = \begin{bmatrix} \frac{1}{r_1} e_{Y,1} K_{X,1} & -\frac{1}{r_2} e_{Y,1} K_{X,1} & & & \\ -\frac{1}{r_1} e_{Y,1} K_{X,1} & \frac{1}{r_2}(e_{Y,1} K_{X,1} + e_{Y,2} K_{X,2}) & -\frac{1}{r_3} e_{Y,2} K_{X,2} & & \\ & -\frac{1}{r_2} e_{Y,2} K_{X,2} & \frac{1}{r_3}(e_{Y,2} K_{X,2} + e_{Y,3} K_{X,3}) & \ddots & \\ & \ddots & \ddots & & -\frac{1}{r_n} e_{Y,n-1} K_{X,n-1} \\ & & & -\frac{1}{r_{n-1}} e_{Y,n-1} K_{X,n-1} & \frac{1}{r_n}(e_{Y,n-1} K_{X,n-1} + e_{Y,n} K_{X,n}) \end{bmatrix}$$

and,

$$[\mathbf{K}_{Y\theta}] = \begin{bmatrix} \frac{1}{r_1} e_{X,1} K_{Y,1} & -\frac{1}{r_2} e_{X,1} K_{Y,1} & & & \\ -\frac{1}{r_1} e_{X,1} K_{Y,1} & \frac{1}{r_2}(e_{X,1} K_{Y,1} + e_{X,2} K_{Y,2}) & -\frac{1}{r_3} e_{X,2} K_{Y,2} & & \\ & -\frac{1}{r_2} e_{X,2} K_{Y,2} & \frac{1}{r_3}(e_{X,2} K_{Y,2} + e_{X,3} K_{Y,3}) & \ddots & \\ & \ddots & \ddots & & -\frac{1}{r_n} e_{X,n-1} K_{Y,n-1} \\ & & & -\frac{1}{r_{n-1}} e_{X,n-1} K_{Y,n-1} & \frac{1}{r_n}(e_{X,n-1} K_{Y,n-1} + e_{X,n} K_{Y,n}) \end{bmatrix}$$

r_i being the radius of gyration of the i^{th} floor about its centre of mass. Further, $\{V_X\}$ (= $\{V_{X1}\ V_{X2}\ ...\ V_{Xi}\ ...\ V_{Xn}\}^T$) and $\{V_Y\}$ (= $\{V_{Y1}\ V_{Y2}\ ...\ V_{Yi}\ ...\ V_{yn}\}^T$) are respectively the relative displacement vectors for the translations along the X and Y-axes, and $\{V_\theta\}$ (= $\{r_1 V_{\theta 1}\ r_2 V_{\theta 2}\ ...\ r_i V_{\theta i}\ ...\ r_n V_{\theta n}\}^T$) is the vector for translations corresponding to the relative rotations about Z-axis.

Let $\{\xi\}$ be the normal coordinates such that the displacements, $\{V\}$ can be defined by the transformation

$$\{V\} = [\Phi]\{\xi\} \qquad (3.3)$$

where, $[\Phi]$ is the modal matrix whose columns are the mode shape vectors, and thus $[\Phi] \equiv [\{\phi^1\}\{\phi^2\}\ ...\ \{\phi^{3n}\}]$. With this transformation and on assuming that the system is classically damped, the system response in the j^{th} mode of vibration may be described by

$$\ddot{\xi}_j + 2\zeta_j \omega_j \dot{\xi}_j + \omega_j^2 \xi_j = -\alpha_j \ddot{Z}_X;\ \mathrm{j} = 1, 2, 3\ ...\ 3n, \qquad (3.4)$$

where, a_j is the modal participation factor expressed as

$$\alpha_j = \frac{\{\phi^j\}^T [M] \{\gamma\}}{\{\phi^j\}^T [M] \{\phi^j\}}, \qquad (3.5)$$

and ζ_j, ω_j respectively are the damping ratio and natural frequency in the j^{th} mode.

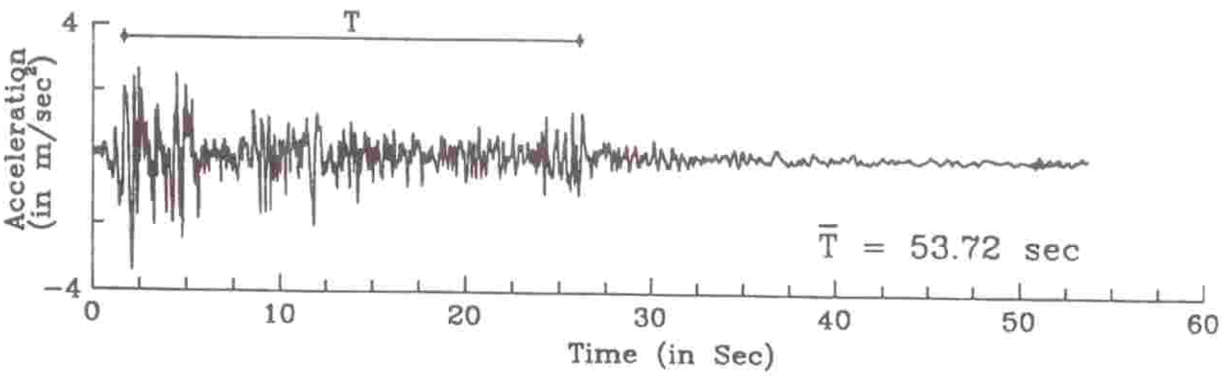

Fig. 3 – Recorded Accelerogram at El Centro Site for Imperial Valley Earthquake, 1940, S00E Component.

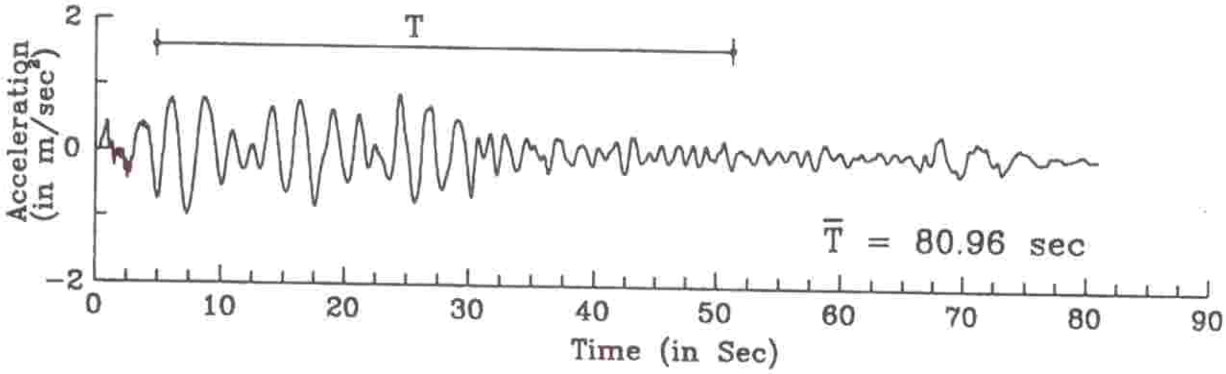

Fig. 4 – Synthetic Accelerogram for Mexico Earthquake, 1985 at Mexico City Site.

4. Energy Spectra for the System Response

Using Eq. (3.3) together with Eq. (3.4), the transfer function, $H(\omega)$ relating the displacement response for the i^{th} degree-of-freedom, $V_i(t)$ to the ground acceleration, $\ddot{Z}_X$ can be written as

$$H(\omega) = \sum_{j=1}^{3n} \phi_{ij}\alpha_j H_j(\omega), \tag{4.1}$$

where, ϕ_{ij} is the i^{th} element of the j^{th} mode shape vector, $\{\phi^j\}$, and

$$H_j(\omega) = \frac{1}{(\omega_j^2 - \omega^2 + 2i\zeta_j\omega_j\omega)}. \tag{4.2}$$

Thus, in frequency domain, the displacement response corresponding to the i^{th} degreeof-freedom becomes

$$V_i(\omega) \quad = H(\omega)Z(\omega)$$

$$= \left(\sum_{j=1}^{3n} \phi_{ij}\alpha_j H_j(\omega)\right) Z(\omega), \tag{4.3}$$

where $Z(\omega)$ is the Fourier transform of $\ddot{Z}_X(t)$. Now, on using this in Eq. (2.3), the energy spectrum of the displacement response becomes

$$ED_i(\omega) = \frac{1}{\pi T}\left| V_i(\omega) \right|^2$$

$$= \frac{1}{\pi T}\left| Z(\omega) \right|^2 \sum_{j=1}^{3n} \sum_{k=1}^{3n} \phi_{ij}\alpha_j\phi_{ik}\alpha_k H_j(\omega) H_k^*(\omega). \tag{4.4}$$

On expanding, this may be written as (as in Gupta and Trifunac (1990a))

$$ED_i(\omega) = \frac{1}{\pi T}\left| Z(\omega) \right|^2 \sum_{j=1}^{3n} \left| H_j(\omega) \right|^2 \Big[\phi_{ij}^2 \alpha_j^2$$

$$+ \sum_{k=1, k\neq j}^{3n} \phi_{ij}\phi_{ik}\alpha_j\alpha_k \left\{ C_{jk} + \left(1 - \frac{\omega^2}{\omega_j^2}\right) D_{jk} \right\} \Big], \tag{4.5}$$

where, C_{jk} and D_{jk} are the coefficients given in terms of ζ_j, ζ_k and r (= ω_k/ω_j) as

$$C_{jk} = \frac{1}{B_{jk}}[8\zeta_j(\zeta_j + \zeta_k r)\{(1-r^2)^2 -$$

$$-4r(\zeta_j - \zeta_k r)(\zeta_k - \zeta_j r)\}] \tag{4.6}$$

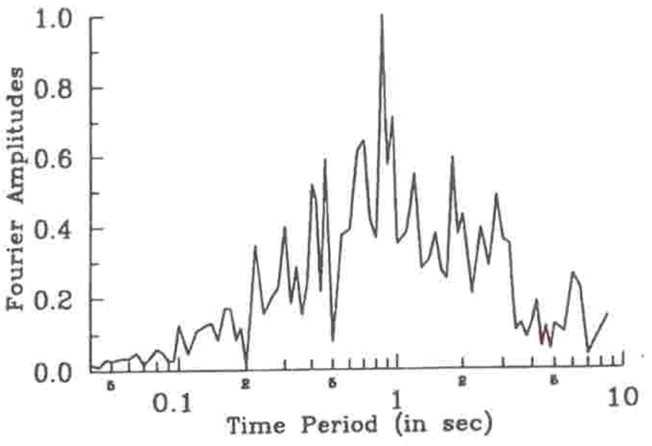

Fig. 5 – Normalized Fourier Spectrum for the Imperial Valley Earthquake.

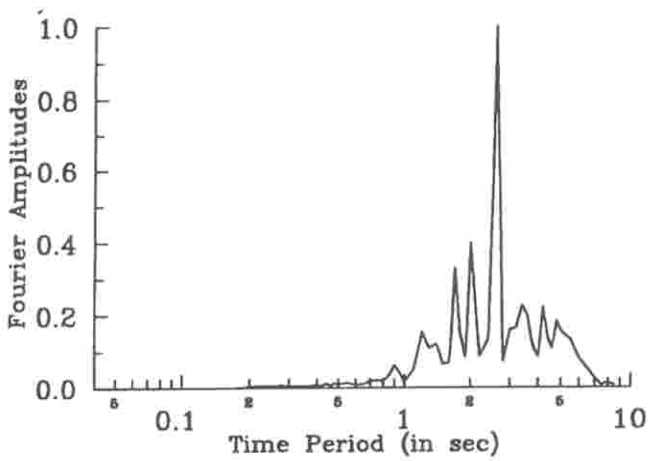

Fig. 6 – Normalized Fourier Spectrum for the Mexico City Earthquake.

$$D_{jk} = \frac{1}{B_{jk}}[2(1-r^2)\{4r(\zeta_j - \zeta_k r) \cdot (\zeta_k - \zeta_j r) - (1-r^2)^2\}] \qquad (4.7)$$

with

$$B_{jk} = 8r^2[(\zeta_j^2 + \zeta_k^2)(1-r^2)^2 - 2(\zeta_k^2 - \zeta_j^2 r^2)(\zeta_j^2 - \zeta_k^2 r^2)] + (1-r^2)^4. \qquad (4.8)$$

In Eq. (4.5), the double summation term can be seen to represent the effects of interaction of the j^{th} mode with the other $n-1$ modes of vibration.

Similarly, the energy spectrum for the torque, $T_i(t)$, about the centre of mass at the i^{th} floor may be obtained as

$$ET_i(\omega) = \frac{1}{\pi T}|Z(\omega)|^2 \sum_{j=1}^{3n} \left|H_j(\omega)\right|^2 \Bigg[\left(\sum_{l=1}^{i} m_l r_l \phi_{(2n+l)_j} \right)^2 \alpha_j^2 \omega_j^4 + \sum_{k=1, k\neq j}^{3n} \left(\sum_{l=1}^{i} m_l r_l f_{(2n+l)_j} \right) \left(\sum_{l=1}^{i} m_l r_l \phi_{(2n+l)_k} \right) \alpha_j \alpha_k \omega_j^2 \omega_k^2 \left\{ C_{jk} + \left(1 - \frac{\omega^2}{\omega_j^2}\right) D_{jk} \right\} \Bigg]. \qquad (4.9)$$

Energy spectra for some more response functions have been given by Agarwal and Gupta (1993).

5. Nonstationarity in the System Response

The above expressions for the energy spectra may be used in Eqs. (2.7) through (2.10) to compute the a_{rms}, ϵ and N values for the desired response function, and then to obtain the amplitude of the desired order of response peak for the given level of confidence by computing the peak factor as in Eq. (2.4) or (2.11). As stated earlier also, the r.m.s. value of the peaks (or of the response function) has to be modified because an earthquake excitation is not a stationary process as it builds up over a small period of time and then decays after remaining stationary for some part of its duration. Some additional nonstationarity is further introduced in the response by virtue of the fact that the dynamical system has a finite operating time. It has been shown by Caughey and Stumpf (1961) that the variance of the response of a singledegree-of-freedom oscillator to a stationary excitation attains the stationary variance value only after a few cycles depending on the frequency and damping of the system. Using Eq. (2.12) for modifying the r.m.s. value may be too simplistic as the value of $\overline{a}$ so computed ignores the correlation between the various modes of vibration. In the present case, these modes may be very close leading to significant degree of correlation. This correlation may be accounted for in a simple but approximate way by scaling $\overline{a}$ as mentioned in Section 2 but in this scheme, it is implicitly assumed that the extent to which nonstationarity affects the response in any mode is not influenced by the extent to which other modes correlate with this mode, and that this extent is same for all the modes. The latter part of this assumption does not appear rational since the degree of nonstationarity may be significantly different in various modal responses due to the different modal frequencies and damping ratios unless the excitation process is very long. In case of the same damping ratio in all the modes, for example, a higher mode may be associated with lesser effect of nonstationarity on the r.m.s. value of the peaks. In view of this, an alternative scheme is proposed here to account for the nonstationarity in a more rational manner.

According to Eq. (4.5), the r.m.s. value of the i^{th} displacement response peaks in the j^{th} mode may be expressed as

$$\overline{a}_j = \left[\frac{2}{\pi T} \phi_{ij}^2 \alpha_j^2 \int_0^\infty |Z(\omega)|^2 \left| H_j(\omega) \right|^2 \mathrm{d}\omega \right]^{1/2}, \qquad (5.1)$$

in the absence of non-stationarity in the response. Due to the effect of nonstationarity, this is modified to $\tilde{a}_j$ which on multiplication with the peak factor, say $\overline{\eta}_j$, gives the largest peak value in the j^{th} mode i.e. $\phi_{ij}\alpha_j SD_j$. SD_j is the spectral displacement corresponding to the modal frequency, ω_j and damping ratio, ζ_j. Thus, the degree of nonstationarity in the j^{th} mode is represented by the ratio $\phi_{ij}\alpha_j SD_j / \overline{\eta}_j \overline{a}_j$, and the r.m.s. value in the

j^{th} mode should be multiplied with this ratio to correct for the nonstationarity. Further, when the modal interaction terms are also included due to the simultaneous vibration in the other modes, the r.m.s. value of the response peaks in the j^{th} mode as in Eq. (5.1) may be considered as modified by the ratio, Γ_j where,

$$\Gamma_j = \left[1 + \left(\sum_{k=1, k\neq j}^{3n} \phi_{ik}\alpha_k C_{jk} \right) / \phi_{ij}\alpha_j \right]^{1/2}. \tag{5.2}$$

Here, the interaction terms involving D_{jk} have been ignored as the function $|H_j(\omega)|^2$ can be approximated by a delta function at $\omega = \omega_j$. Thus, for considering the modal correlation also, the r.m.s. value of the peaks in the j^{th} mode may be taken as $\phi_{ij}\alpha_j\Gamma_j SD_j / \overline{\eta}j$, or in other words, the largest peak value in the j^{th} mode may be taken as $\phi_{ij}\alpha_j\Gamma_j SD_j$. Based on this logic, it is proposed that the scheme suggested by Gupta and Trifunac (1987b) may be adopted here. However, for computing the modified r.m.s. value of peaks as in Eq. (2.12), the largest peak value in the j^{th} mode may be taken, for example, as

$$D_{ij} = SD_j \left(\phi_{ij}^2 \alpha_j^2 + \sum_{k=1, k\neq j}^{3n} \phi_{ij}\phi_{ik}\alpha_j\alpha_k C_{jk} \right)^{\frac{1}{2}}, \tag{5.3}$$

and

$$T_{ij} = SD_j \left[\left(\sum_{l=1}^{i} m_l r_l \phi_{(2n+l)j} \right)^2 \alpha_j^2 \omega_j^4 + \sum_{k=1, k\neq j}^{3n} \left(\sum_{l=1}^{i} m_l r_l \phi_{(2n+l)j} \right) \left(\sum_{l=1}^{i} m_l r_l \phi_{(2n+l)k} \right) \alpha_j \alpha_k \omega_j^2 \omega_k^2 C_{jk} \right]^{\frac{1}{2}}, \tag{5.4}$$

respectively for the responses, $V_i(t)$ and $T_i(t)$ at the i^{th} floor.

6. Illustration of the Proposed Model

Two fixed-base multistoried buildings have been considered here for the illustration of the approach formulated above. The first example building is a 7-story building having non-uniform floor dimensions, 26 × 33 m for the bottom three stories and 20 × 25 m for the remaining four stories at the top. Each story is of 3.75 m height. The second building is a 15-story building with the uniform floor dimensions of 25 × 100 m at each floor level, and with the constant story height of 5.0 m. The translational stiffnesses in the X-direction for both the buildings are different from those in the Y-direction, and these also vary from story to story. Further, the static eccentricities in either direction are different from floor to floor, and thus, the centres of stiffness at various floors are not lying on a vertical straight line. In case of the second building, eccentricities in the X and Y-directions at all the floor levels have been taken to be same. Various properties of these example buildings are shown in Tables 1 and 2. The torsional stiffnesses of various stories have been computed in these tables by neglecting the contributions of the torsional stiffnesses of the various supporting structural elements about their own longitudinal axes. The natural frequencies of these buildings are shown in Tables 3 and 4. It may be observed that modes in both the example buildings are quite closely spaced with the frequency ratio being about 1.15 in the lower, and as low as 1.03 in the higher adjacent modes. The critical damping ratio has been assumed same as 0.05 in all the modes of vibration for both the buildings.

Two earthquake excitations with the following characteristics have been considered here for the purpose of illustration:

1. Recorded motion, S00E component, at El Centro site during the Imperial Valley Earthquake, 1940.
2. Synthetically generated motion for the Mexico Earthquake, 1985 at Mexico City Site (as in Gupta and Trifunac (1990c)).

The accelerograms for these motions and the corresponding Fourier spectra (as normalized with respect to their maximum amplitudes) have been shown in Figs. 3 to 6. It may be observed that the first example excitation is of broad band nature with the distribution of energy in the broad range of 0.2-5 sec. Significant frequencies of both the buildings lie in this range. However, the second excitation is of narrow band nature with the concentration of energy at the periods close to 2.5 sec. The example buildings (particularly the first one) are quite stiff compared to this, and therefore, this excitation should cause significant degrees of input-dependent modal correlation in the building responses (Singh and Mehta (1983), Gupta (1990)). Further, since the time duration, T should correspond to the stationary part of the excitation, not to the actual record length, $\overline{T}$, it has been assumed to be that time interval during which 90% of the total energy arrives after the initial arrival of 5% (see Trifunac and Brady (1975)). Therefore, the value of T for these example excitations has been taken as 24.44 sec and 46.44 sec respectively (instead of $\overline{T}$ = 53.72 and 80.96 sec).

A deterministic time domain analysis based on the step-by-step numerical integration has been carried out here for both example buildings under the ground accelerations as in Figs. 3 and 4. Its results have been compared with the results of the proposed stochastic approach by plotting the envelopes of the largest peak displacements as shown in Figs. 7 to 10. The results of the stochastic approach consist of the expected values and the values corresponding to the 5% and 95% probabilities of exceedance. In each figure, the response values have been normalized with respect to the respective overall maximum response values. It is seen from these figures that irrespective of the relative stiffnesses of the buildings to the excitations, the "expected" system responses based on the stochastic approach are in good agreement with the time domain analysis results. Further, the time analysis estimates are also bounded on either side by the 5% or 95% confidence level estimates. Similar results are also obtained in case of the

Floor Level, i	Mass m_i	Radius of Gyration, r_i	Stiffnesses K_{xi}	K_{yi}	$K_{\theta i}$	Eccentricities e_{xi}	e_{yi}
1	$0.80m$	r	$2.212k$	$1.392k$	$1.680kr^2$	$0.20r$	$0.26r$
2	$0.80m$	r	$2.696k$	$2.179k$	$2.311kr^2$	$0.20r$	$0.26r$
3	$0.80m$	r	$3.100k$	$2.697k$	$2.837kr^2$	$0.20r$	$0.26r$
4	$0.80m$	r	$3.424k$	$3.112k$	$3.257kr^2$	$0.24r$	$0.26r$
5	$1.15m$	$1.3r$	$4.998k$	$4.792k$	$11.094kr^2$	$0.34r$	$0.50r$
6	$1.15m$	$1.3r$	$5.240k$	$5.083k$	$11.718kr^2$	$0.34r$	$0.50r$
7	$1.15m$	$1.3r$	$5.361k$	$5.229k$	$12.878kr^2$	$0.34r$	$0.50r$

$m = 1 \times 10^6$ kg, $k = 1 \times 10^9$ N/m, $r = 9.242$ m.

Table 1 – Properties of First Example Building

Floor Level, i	Mass m_i	Radius of Gyration, r_i	Stiffnesses K_{xi}	K_{yi}	$K_{\theta i}$	Eccentricities e_{xi}	e_{yi}
1	$0.60m$	r	$0.600k$	$0.793k$	$1.014kr^2$	$0.060r$	$0.060r$
2	$0.63m$	r	$0.623k$	$0.824k$	$1.053kr^2$	$0.063r$	$0.063r$
3	$0.66m$	r	$0.652k$	$0.863k$	$1.102kr^2$	$0.066r$	$0.066r$
4	$0.69m$	r	$0.681k$	$0.901k$	$1.151kr^2$	$0.069r$	$0.069r$
5	$0.72m$	r	$0.710k$	$0.939k$	$1.200kr^2$	$0.072r$	$0.072r$
6	$0.74m$	r	$0.739k$	$0.978k$	$1.249kr^2$	$0.075r$	$0.075r$
7	$0.77m$	r	$0.768k$	$1.016k$	$1.298kr^2$	$0.077r$	$0.077r$
8	$0.80m$	r	$0.797k$	$1.054k$	$1.347kr^2$	$0.080r$	$0.080r$
9	$0.83m$	r	$0.826k$	$1.093k$	$1.396kr^2$	$0.083r$	$0.083r$
10	$0.86m$	r	$0.855k$	$1.131k$	$1.445kr^2$	$0.086r$	$0.086r$
11	$0.89m$	r	$0.884k$	$1.170k$	$1.494kr^2$	$0.089r$	$0.089r$
12	$0.91m$	r	$0.913k$	$1.208k$	$1.543kr^2$	$0.092r$	$0.092r$
13	$0.94m$	r	$0.942k$	$1.246k$	$1.592kr^2$	$0.095r$	$0.095r$
14	$0.97m$	r	$0.971k$	$1.213k$	$1.641kr^2$	$0.097r$	$0.097r$
15	$1.00m$	r	$1.000k$	$1.323k$	$1.690kr^2$	$0.100r$	$0.100r$

$m = 0.792 \times 10^6$ kg, $k = 1.971 \times 10^9$ N/m, $r = 29.76$ m.

Table 2 – Properties of Second Example Building

Mode #	ω_n (rad/sec)	Mode #	ω_n (rad/sec)
1	12.49	12	77.27
2	14.63	13	88.52
3	18.87	14	91.23
4	29.21	15	96.62
5	34.99	16	100.39
6	42.74	17	108.54
7	45.81	18	113.41
8	55.81	19	122.41
9	63.11	20	129.43
10	67.53	21	156.98
11	75.27		

Table 3 – Natural Frequencies of First Example Building

Mode #	ω_n (rad/sec)	Mode #	ω_n (rad/sec)	Mode #	ω_n (rad/sec)
1	5.55	16	54.35	31	93.24
2	6.34	17	56.35	32	95.54
3	7.35	18	57.30	33	96.01
4	15.00	19	64.92	34	96.78
5	17.16	20	65.06	35	97.70
6	19.81	21	65.63	36	102.28
7	24.32	22	72.23	37	104.21
8	27.82	23	74.40	38	106.64
9	32.08	24	75.68	39	109.80
10	33.05	25	78.90	40	111.74
11	37.80	26	82.72	41	111.78
12	41.20	27	84.62	42	118.12
13	43.58	28	85.95	43	123.15
14	47.15	29	89.43	44	126.79
15	49.25	30	90.23	45	129.13

Table 4 – Natural Frequencies of Second Example Building

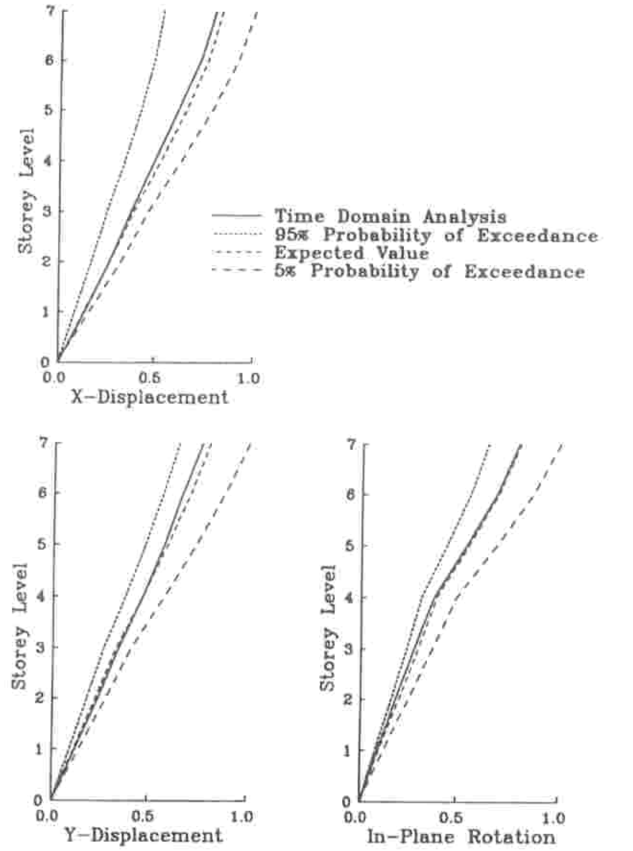

Fig. 7 – Normalized Displacement Responses in First Example Building for Imperial Valley Earthquake.

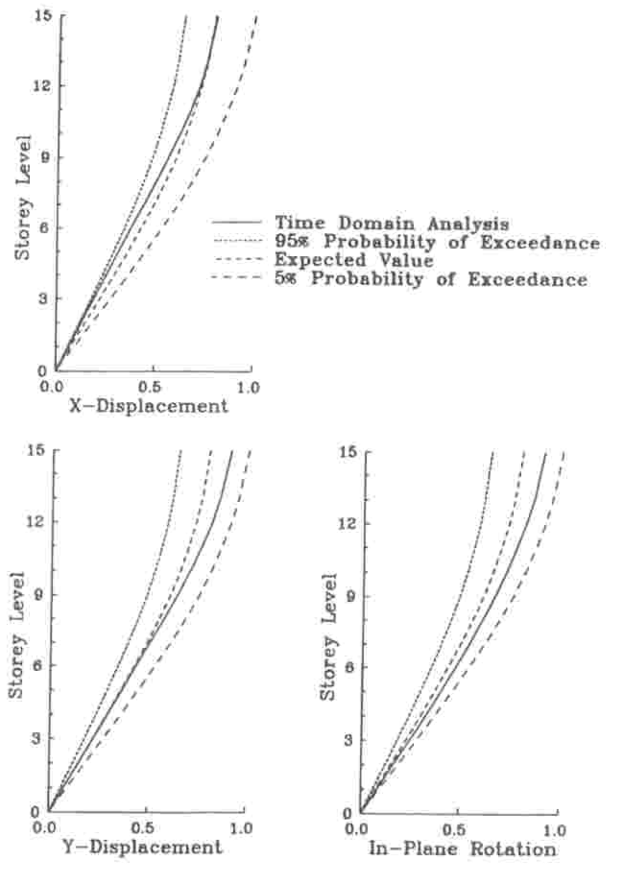

Fig. 8 – Normalized Displacement Responses in Second Example Building for Imperial Valley Earthquake.

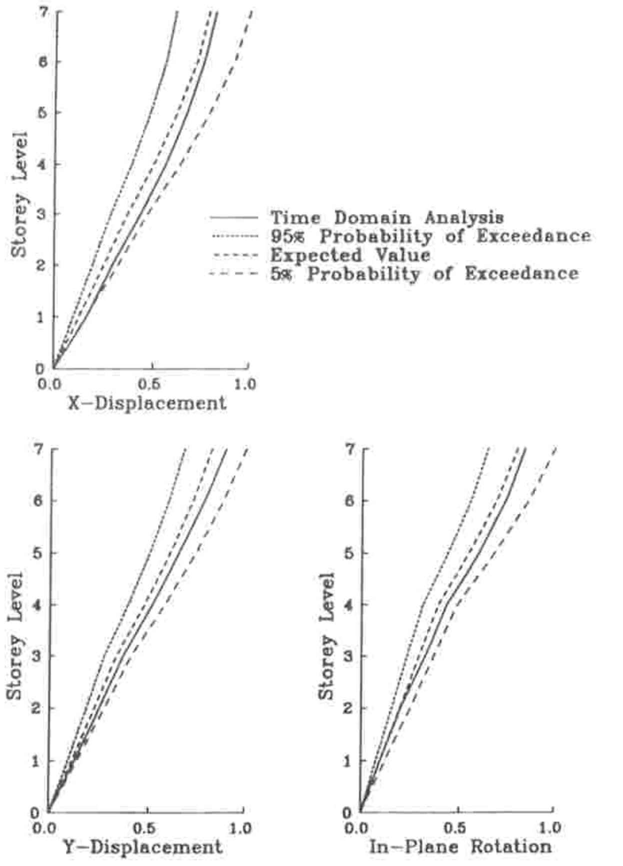

Fig. 9 – Normalized Displacement Responses in First Example Building for Mexico Earthquake.

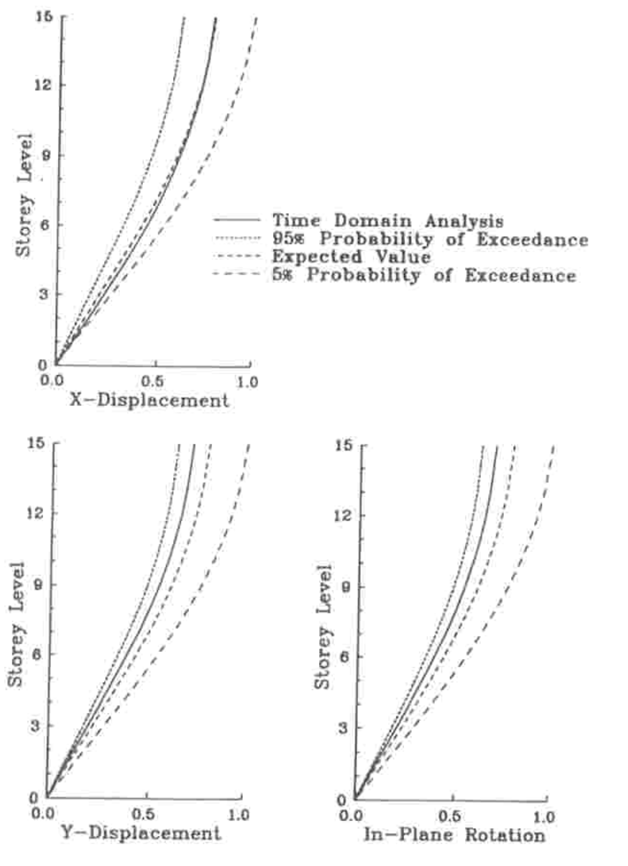

Fig. 10 – Normalized Displacement Responses in Second Example Building for Mexico Earthquake.

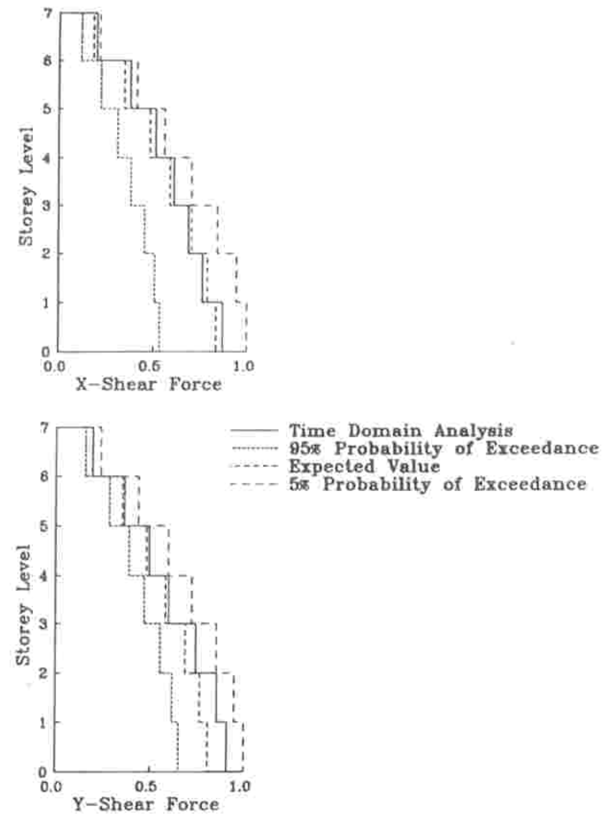

Fig. 11 – Normalized Shear Responses in First Example Building for Imperial Valley Earthquake.

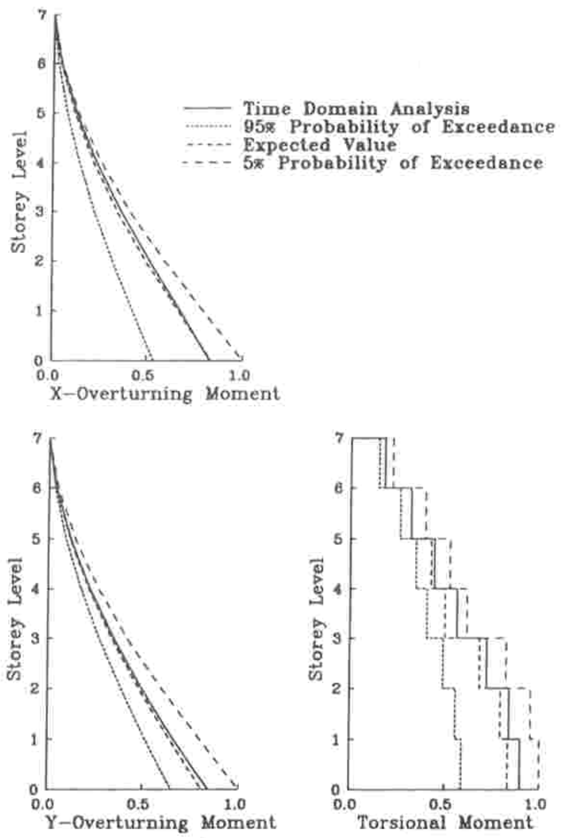

Fig. 12 – Normalized Moment Responses in First Example Building for Imperial Valley Earthquake.

shear force, overturning moment and torsional moment responses. For example, Figs. 11 and 12 show the comparison of the envelopes of these responses for the first example building under the Imperial Valley excitation. These and some more results as in Agarwal and Gupta (1993) confirm the ability of the proposed formulation to account for the effects of modal correlation, whether those are due to the closeness of modes or due to the nature of the input excitation, in a reasonably accurate manner.

7. Conclusions

A response spectrum based stochastic approach has been formulated for the linear seismic response of fixed-base, torsionally coupled multistoried buildings. This approach uses the information available from the Fourier synthesis of the ground motion, and from this, the estimates of response peaks for all orders can be obtained with the desired level of confidence. It is possible to obtain the expected peak values of any response function by using this approach, and thus to get an idea about the 'average' values which the response function may assume during the life time of the building. Further, depending on the importance of the structure and its intended life, suitable design values can be obtained by choosing an appropriate probability of exceedance.

The presented formulation accounts for the cross-correlation between the various modes of vibration in a simple way, by including the effects of interaction terms in the peak modal responses. As shown by the results for the considered example buildings and ground motions, this approach is applicable to the frequently encountered cases of closely spaced modes in the torsionally coupled buildings, even under the excitation by the narrow-band, long period motions. This can be easily extended to the case of the multi-component excitation also with the knowledge of the correlations between the different components.

References

Agarwal, P. and V.K. Gupta (1993). Stochastic response of torsionally coupled multistoreyed buildings, *Report No. 93-01, Dept. Civil Eng, I.I.T. Kanpur, India.*

Amini, A. and M.D. Trifunac (1981). Distribution of peaks in linear earthquake response, *J. Eng. Mech. Div., Proc. ASCE*, **107(EM1)**, 207-227.

Amini, A. and M.D. Trifunac (1985). Statistical extension of response spectrum superposition, *Soil Dyn. Earthq. Eng.*, **4(2)**, 54-63.

Basu, B. and V.K. Gupta (1994). A probabilistic assessment of seismic damage in ductile structures, *Submitted for publication.*

Basu, B., V.K. Gupta, and D. Kundu (1994). A study on ordered peaks in seismic damage analysis, *Re-*

port No. 94-01, Dept. Civil Eng., I.I.T. Kanpar, India.

Cartwright, D.E. and M.S. Longuet-Higgins (1956). The statistical distribution of maxima of a random function, *Proc. Roy. Soc. London*, **A 237**, 212-232.

Caughey, T.K. and H.J. Stumpf (1961). Transient response of a dynamic system under random excitation, *J. Appl. Mech.* (ASME), **28E(4)**, 563-566.

Chandler, A.M. (1986). Building damage in Mexico City earthquake, *Nature*, **320(6062)**, 497-501.

Chandler, A.M. and G.L. Hutchinson (1986). Seismic design eccentricity for torsionally coupled building, *Proc. Eighth Eur. Conf. Earthq. Eng., Lisbon*, **6(7)**, 33-40.

Chandler, A.M. and G.L. Hutchinson (1987). Evaluation of code torsional provisions by a time history approach, *Earthq. Eng. Struct. Dyn.*, **15**, 491-516.

David, F.N. and N.L. Johnson (1954). Statistical treatment of censored data, Part I: Fundamental formulae, *Biometrika*, **41**, 228-240.

Dempsey, K.M. and H.M. Irvine (1979). Envelopes of maximum seismic response for a partially symmetric single-storey building model, *Earthq. Eng. Struct. Dyn.*, **7**, 161-180.

Dempsey, K.M. and W.K. Tso (1982). An alternative path to seismic torsional provisions, *Soil Dyn. Earthq. Eng.*, **1(1)**, 3-10.

Douglas, B.M. and T.E. Trabert (1973). Coupled torsional dynamic analysis of a multistory building, *Bull. Seism. Soc. Amer.*, **63(3)**, 1025-1039.

Gibson, R.E., M.L. Moody and R.S. Ayre (1972). Response spectrum solution for earthquake analysis of unsymmetrical multistoried building, *Bull. Seism. Soc. Amer.*, **62**, 215-229.

Gupta, I.D. and M.D. Trifunac (1987a). A note on contribution of torsional excitation to earthquake response of simple symmetric buildings, *Earthq. Eng. Eng. Vib.*, **7(3)**, 27-46.

Gupta, I.D. and M.D. Trifunac (1987b). Order statistics of peaks in earthquake response of multi-degree-of-freedom systems, *Earthq. Eng. Eng. Vib., 7(4)*, 15-50.

Gupta, I.D. and M.D. Trifunac (1988). Order statistics of peaks in earthquake response, *J. Eng. Mech. (ASCE)*, **114(10)**, 1605-1627.

Gupta, V.K. (1990). New ideas on response spectrum superposition and modal interaction. *Ninth Sym. Earthg. Eng., Roorkee, India*, **1(2)**, 43-50.

Gupta, V.K. (1994). Stochastic approach to seismic floor spectra in nuclear power plants, *Report No. 94-02, Dept. Civil Eng., I.I.T. Kanpur, India.*

Gupta, V.K. and M.D. Trifunac (1990a). Response of multistoried buildings to ground translation and torsion during earthquakes, *European Earthq. Eng.*, **IV(1)**, 34-42.

Gupta, V.K. and M.D. Trifunac (1990b). A note on contribution of ground torsion to seismic response of symmetric multistoried buildings, *Earthq. Eng. Eng. Vib.*, **10(3)**, 27-40.

Gupta, V.K. and M.D. Trifunac (1990c). Response of multistoried buildings to ground translation and rocking during earthquakes, *J. Prob. Eng. Mech.*, **5(3)**, 138-145.

Gupta, V.K. and M.D. Trifunac (1991). Seismic response of multistoried buildings including the effects of soil-structure interaction, *Soil Dyn. Earthq. Eng.*, **10(8)**, 414-422.

Hejal, R. and A.K. Chopra (1989a). Earthquake analysis of a class of torsionally-coupled buildings, *Earthq. Eng. Strect. Dyn.*, **18**, 305-323.

Hejal, R. and A.K. Chopra (1989b). Earthquake response of torsionally coupled, frame buildings, *J. Struct. Eng. (ASCE)*, **115(4)**, 834-851.

Hutchinson, G.L., A.M. Chandler and M.A. Rady (1991). Effect of vertical distributions of mass and translational stiffness on dynamic eccentricities for a special class of multistorey buildings, *Pacific Conf. Earthq. Eng., New Zealand*, **1**, 61-69.

Kan, C.L. and A.K. Chopra (1977a). Effects of torsional coupling on earthquake forces in buildings, *J. Strect. Div., Proc. ASCE*, **103(ST4)**, 805-819.

Kan, C.L. and A.K. Chopra (1977b). Elastic earthquake analysis of torsionally coupled multistorey buildings, *Earthq. Eng. Struct. Dyn.*, **5**, 395-412.

Keintzel, E. (1973). On the seismic analysis of unsymmetrical storied buildings, *Proc. Eighth. Wld Conf. Earthq. Eng, Rome*, **Paper 10**, 110-113.

Kung, S.Y. and D.A. Pecknold (1984). Seismic response of torsionally coupled singlestorey structures, *Proc. Eighth Wld Conf. Earthq. Eng., San Francisco, California*, 235-242.

Lam, P.C. and R.J. Scavuzzo (1981). Lateral-torsional structural response from freefield ground motion, *Nucl. Eng. Design*, **65**, 269-281.

Maheri, M.R., A.M. Chandler and R.H. Bassett (1991). Coupled lateral-torsional behaviour of frame structures under earthquake loading, *Earthq. Eng. Strect. Dyn.*, **20**, 61-45.

Mohraz, B. and F.E. Elghadamsi (1989). Earthquake ground motion and response spectra, *Seismic Design Handbook, Van Nostrand Reinhold. New York*, 32-80.

Penzien, J. (1969). Earthquake response of irregularly shaped buildings, *Proc. Fourth Wld Conf. Earthq. Eng., Santiago, Chile*, **II(A-3)**, 75-89.

Rady, M.A. and G.L. Hutchinson (1988). Evaluation of dynamic eccentricities obtained using a probabilistic approach, response spectrum methods and modern building codes, *Earthq. Eng. Struct. Dyn.*, **16**, 275-291.

Rice, S.O. (1944). Mathematical analysis of random noise, *Bell Syst. Tech. J.*, **23**, 282-332.

Rice, S.O. (1945). Mathematical analysis of random noise, *Bell Syst. Tech. J.*, **24**, 46-156.

Rutenberg, A., T.-I. Hsu and W.K. Tso (1978). Response spectrum techniques for asymmetric buildings, *Earthq. Eng. Strect. Dyn.*, **6**, 427-435.

Singh, M.P. and K.B. Mehta (1983). Seismic design response by an alternative SRSS rule, *Earthq. Eng. Struct. Dyn.*, **11**, 771-783.

Trifunac, M.D. and A.G. Brady (1975). A study on the duration of strong earthquake ground motion, *Bull. Seism. Soc. Amer.*, **65(3)**, 581-626.

Tsicnias, T.G. and G.L. Hutchinson (1981). Evaluation of code requirements for the earthquake resistant design of torsionally coupled buildings, *Proc. Instn. Civ. Engrs.*, **Part 2** (**71**), 821-843.

Tsicnias, T.G. and G.L. Hutchinson (1982a). Evaluation of code torsional provisions for earthquake resistant design of single storey buildings with two eccentricity components, *Proc. Instn. Civ. Engrs.*, **Part 2** (**73**), 455-464.

Tsicnias, T.G. and G.L. Hutchinson (1982b). A note on the perturbation analysis of the mode shapes of torsionally coupled buildings, *Earthq. Eng. Struct. Dyn.*, **10**, 171-174.

Tso, W.K. and K.M. Dempsy (1980). Seismic torsional provisions for dynamic eccentricity, *Earthq. Eng. Struct. Dyn.*, **8**, 275-289.

Udwadia, F.E. and M.D. Trifunac (1973). Fourier transforms, response spectra and their relationship through the statistics of oscillator response, *Report EERL 73-01, California Institute of Technology, Pasadena, California.*

Udwadia, F.E. and M.D. Trifunac (1974). Characterization of response spectra through the statistics of oscillator response, *Bull. Seism. Soc. Amer.*, **64**, 205-219.